MOLECULAR AND CELLULAR BIOLOGY, Mar. 1993, p. 1686–1696
0270-7306/93/031686-11$02.00/0

Vol. 13, No. 3

# T Cell Receptor-β mRNA Splicing: Regulation of Unusual Splicing Intermediates

LIAN QIAN,[1] LIVIA THEODOR,[1]† MARK CARTER,[1] MINH N. VU,[1] ANNA W. SASAKI,[2] AND MILES F. WILKINSON[1]*

*Microbiology and Immunology Department, L220, Vollum Institute for Advanced Biomedical Research,[1] and Department of Medicine and V.A. Medical Center,[2] Oregon Health Sciences University, 3181 S.W. Sam Jackson Park Road, Portland, Oregon 97201*

Received 15 July 1992/Returned for modification 1 October 1992/Accepted 18 December 1992

**The expression of functional T cell receptor-β (TCR-β) transcripts requires the activation of programmed DNA rearrangement events. It is not clear whether other mechanisms dictate TCR-β mRNA levels during thymic ontogeny. We examined the potential role of RNA splicing as a regulatory mechanism. As a model system, we used an immature T cell clone, SL12.4, that transcribes a fully rearranged TCR-β gene but essentially lacks mature 1.3-kb TCR-β transcripts in the cytoplasm. Abundant TCR-β splicing intermediates accumulate in the nucleus of this cell clone. These splicing intermediates result from inefficient or inhibited excision of four of the five TCR-β introns; the only intron that is efficiently spliced is the most 5′ intron, $IVS_L$. The focal point for the regulation appears to be $IVS1_{C\beta1}$ and $IVS2_{C\beta1}$, since unusual splicing intermediates that have cleaved the 5′ splice site but not the 3′ splice site of these two introns accumulate in vivo. The block in 3′ splice site cleavage is of interest since sequence analysis reveals that these two introns possess canonical splice sites. A repressional mechanism involving a labile repressor protein may be responsible for the inhibition of RNA splicing since treatment of SL12.4 cells with the protein synthesis inhibitor cycloheximide reversibly induces a rapid and dramatic accumulation of fully spliced TCR-β transcripts in the cytoplasm, concomitant with a decline in TCR-β pre-mRNAs in the nucleus. This inducible system may be useful for future studies analyzing the underlying molecular mechanisms that regulate RNA splicing.**

The T cell receptor (TCR) for antigen is a multisubunit receptor composed of two variable chains that recognize antigen (either the TCR-α and -β or TCR-γ and -δ subunits) and several CD3 invariant chains that are involved in signal transduction (2). TCR-β chains are of particular interest for several reasons, including the fact that they recognize so-called superantigens found in the natural environment (18). TCR-β proteins are encoded by gene segments that have undergone DNA rearrangement events. TCR-β genes that have juxtaposed $D_\beta$ and $J_\beta$ elements (partial rearrangement) or have remained unrearranged can transcribe a truncated (1.0-kb) mRNA molecule of unknown function (24). Fully rearranged TCR-β genes that have joined a $V_\beta$ gene segment to either $D_\beta J_\beta$ or $J_\beta$ give rise to full-length (1.3-kb) mature TCR-β transcripts that can encode a functional TCR-β protein (24).

The expression of TCR-β transcripts during T cell maturation has been well studied. Truncated (1.0-kb) TCR-β transcripts are expressed very early in murine ontogeny (at least as early as day 14 of mouse gestation) along with CD3-γ, -δ, -ε, and -ζ transcripts (11, 16, 42). Full-length (1.3-kb) TCR-β transcripts are not evident until days 15 to 16 of mouse gestation. Since this is approximately the same point of gestation when fully rearranged TCR-β genes are detectable (16, 42), it is widely assumed that the first expression of functional TCR-β transcripts is limited by gene rearrangement events. As ontogeny proceeds, the level of 1.3-kb TCR-β mRNA increases in the thymus. This increase is, at least in part, due to the fact that increasing numbers of thymocytes undergo rearrangement events in the thymus, but it also may be due to alterations in transcriptional or posttranscriptional regulatory events. On day 17, TCR-α transcripts become apparent in the fetal thymus (11, 42). This event roughly coincides with the appearance of cell surface TCR-αβ protein on a small proportion of fetal thymocytes (42). Thus, the TCR-α chain appears to be the limiting subunit that controls the surface expression of TCR-αβ protein early in ontogeny. TCR-β protein has also been detected on the surface of immature thymocytes or cell lines in the absence of the TCR-α chain (21, 33), but its function in this context is not yet known.

The transcriptional regulation of the TCR-β gene has been studied in cell culture. A tissue-specific enhancer element has been defined 3′ of the $C_{\beta2}$ gene segment (23, 29). *cis*-acting elements important for TCR-β expression have also been characterized in $V_\beta$ promoters and the J-$C_{\beta2}$ intron region. DNA-binding proteins that possess strong affinity for these regulatory elements have been identified, some of which may be involved in programmed DNA rearrangement events rather than transcriptional regulation per se (17, 20, 25, 37, 44). Negative *trans*-acting factors that serve to inhibit the transcription of TCR-β and other T cell genes that are normally activated during intermediate stages of thymic development have been identified in immature T cell clones (26, 50).

The importance of posttranscriptional mechanisms in regulating TCR-β expression or function is not clear. TCR-β transcripts appear to be capable of undergoing alternative splicing events, but the functional significance of the known examples of alternative splicing is not known. An alternative $C_\beta$ exon ($C_{\beta0}$) present in the J-$C_{\beta1}$ intron is utilized in only a minority of mouse TCR-β mature transcripts and is not present in either rat or human TCR-β genes (4, 9). Alterna-

* Corresponding author.
† Present address: Department of Life Sciences, Bar-Ilan University, Tel Aviv, Israel.

TABLE 1. Oligonucleotides

| Name | Orientation | Position[a] | Sequence | Reference |
|---|---|---|---|---|
| E1 | Antisense | Exon 1, 27–49[b] | GAGAGCTCAAACAAGGAGACCTT | 14 |
| E2 | Antisense | Exon 2, 1–17 | TGAGGTAATCCCACAGT | 14 |
| E2′ | Sense | Exon 2, 1–18 | ACTGTGGGATTACCTCAG | 14 |
| E3 | Antisense | Exon 3, 1–16[c] | CCTTGTTGATAGGATGC | 14 |
| E3B | Antisense | Exon 3, 87–107 | CATAGCCATCACCACCAGTGT | 14 |
| I1 | Antisense | IVS1, 1–19 | CTCCCCAGGTCCCACTTAC | 14 |
| I1B | Antisense | IVS1, 475–491 | GGAAAATGGATGAGACC | 14 |
| I1′ | Sense | IVS1, 17–33 | GAGCTGGCAAGAAGAAT | 14 |
| V | Antisense | $V_{\beta5.1}$, 1–14[d] | CAGAATTTGCTGAACCTGGG | 8 |
| V′ | Sense | L-$V_{\beta5.1}$, 63–79[e] | CTTTCTCCTGGGAACAAGT | 8 |

[a] Position number is determined from start of exon or intron, unless otherwise noted.
[b] Two-nucleotide mismatch to generate a *Sac*I restriction site.
[c] Includes one nucleotide of IVS2.
[d] Includes five nucleotides of IVS-L.
[e] Includes two nucleotides of IVS-L (position number is determined from the translation start site).

tive splicing of $V_\beta$ leader exons has been observed (8), but this does not appear to be a general phenomenon.

As a model system with which to study the parameters that regulate TCR-β mRNA levels, we have used a set of related murine AKR T-lymphoma cell clones that have been carefully phenotyped and shown to represent distinct stages of thymic development. The SL12.4 cell clone has been the subject of many of our studies on T cell gene regulation (26, 50, 51). SL12.4 cells have a surface phenotype ($CD3^-$ $CD4^-$ $CD8^-$ $IL2R\alpha^+$ $HSA^+$ $CD44^-$ $Thy1^+$) that is characteristic of intermediate-maturity thymocytes within the double-negative subset that have a high potential to differentiate into mature T cells in organ culture or after adoptive intrathymic transfer (40). SL12.4 cells accumulate CD3-γ, -δ, -ε, and -ζ mRNAs and possess fully rearranged TCR-α and -β genes, but they do not express the TCR/CD3 complex on their surface (26, 50, 51). In this report, we show that SL12.4 cells transcribe a fully rearranged TCR-β gene but fail to accumulate mature TCR-β transcripts in the cytoplasm. Instead, conventional and unusual intron-containing TCR-β transcripts accumulate in the nucleus of these cells. The splicing of these transcripts may be inhibited by a labile protein(s) since the protein synthesis inhibitor cycloheximide (CHX) induces a dramatic accumulation of fully spliced TCR-β transcripts in the cytoplasm of these cells.

## MATERIALS AND METHODS

**RNA preparation and Northern (RNA) blots.** Total cellular RNA was prepared by lysis in guanidinium isothiocyanate, followed by ultracentrifugation over a 5.7 M CsCl cushion, as described previously (reference 48, protocol 1). Cytoplasmic and nuclear RNA were prepared as described previously (reference 48, protocols 6 and 7). Briefly, the cells were lysed in a Tris-saline buffer containing 0.5% Nonidet P-40, 0.25% sodium deoxycholate, and 50 μg of dextran sulfate per ml and then immediately centrifuged to generate a nuclear pellet and a cytoplasmic supernatant; these two fractions were completely denatured in guanidinium isothiocyanate buffer, and the RNA was prepared as described for the total cellular RNA. Poly(A)$^+$ RNA was prepared directly from cell lysates as described previously (reference 48, protocol 9). RNase H mapping was performed as follows. RNA was first incubated with 5 μM oligonucleotide in 10 mM Tris (pH 7.6)–1 mM EDTA in a total volume of 10 μl for 30 min at 45°C, and then 15 μl of an RNase H cocktail that consisted of 2.5 μl of 10× RNase H buffer (0.2 M *N*-2-hydroxyethylpiperazine-*N*′-2-ethanesulfonic acid [HEPES; pH 8.0], 0.5 M KCl, 0.1 M $MgCl_2$), 2.5 μl of 10 mM dithiothreitol, 1 U of RNase H, and $H_2O$ was added. After incubation in this cocktail for 20 min at 37°C, the RNA was extracted and ethanol precipitated.

RNA was electrophoresed in agarose gels in the presence of formaldehyde and morpholinepropanesulfonic acid (MOPS) and then capillary blotted onto Nytran membranes (38). RNA was also electrophoresed in denaturing polyacrylamide gels containing 7 M urea and 1× Tris-borate-EDTA (38). The RNA from polyacrylamide gels was electroblotted onto Nytran membranes in 10 mM Tris (pH 7.8)–5 mM sodium acetate–0.5 mM EDTA overnight at 50 mA and then for 1 h at 200 mA. All blots were stained with methylene blue (49) to demonstrate equivalent loading of RNA and to mark the migration of rRNA transcripts and RNA molecular weight ladders (Bethesda Research Laboratories). The blots were hybridized with random oligomer-primed $^{32}P$-labeled cDNA inserts in the presence of 10% dextran sulfate and 50% formamide for 12 to 18 h at 42°C (38). Hybridization with single-stranded riboprobes was performed by overnight incubation at 60°C in a buffer containing 5× SSPE (1× SSPE is 0.18 M NaCl, 10 mM $NaPO_4$, and 1 mM EDTA [pH 7.7]), 5× Denhardt's solution, 5 mM EDTA, 0.1% sodium pyrophosphate, 0.5% sodium dodecyl sulfate (SDS), 50 μg of sheared salmon sperm DNA per ml, and 50% formamide (see reference 38 for recipes). All blots were briefly washed at room temperature with 1× SSPE–0.1% SDS and then subjected to several longer washes with 0.1× SSPE–0.1% SDS–5 mM EDTA at 50 to 60°C. Blots were stripped for sequential hybridization by placing them in boiling 0.1× SSPE–0.1% SDS and then gently agitating them while they cooled to room temperature.

Densitometry was performed on XAR-5 film, using a Helana Laboratories model Quick Scan R & D. The densitometer was shown to provide linear values from autoradiographs exposed to a 30-fold range of known amounts of $^{32}P$.

**Oligonucleotides, DNA probes, PCR, and DNA sequencing.** The oligonucleotides used are described in Table 1. $IVS1_{C\beta1}$ (0.5-kb) and $IVS2_{C\beta1}$ (0.13-kb) DNA fragments were prepared by the polymerase chain reaction (PCR) with a murine $C_{\beta1}$ genomic template (14) and the oligonucleotide pairs I1/I1′ and E2′/E3, respectively. The $IVS_{V\beta5.1\text{-}L}$ (0.15-kb) fragment was amplified from $V_{\beta5.1}$ genomic DNA (8) by using the oligonucleotide pair V/V′. The following probes were generated by restriction endonuclease cleavage and gel purification (35): $IVS3_{C\beta1}$ (0.15-kb *Nco*I-*Hin*fI fragment);

$IVS_{JC\beta1}$ (0.75-kb *Eco*RI-*Kpn*I fragment just 5′ of $C_{\beta1}$); $C_{\beta1}$ exon 4 (0.3-kb *Eco*RI-*Hin*dIII fragment from the 3′ untranslated region); $C_{\beta2}$ exon 4 (0.2-kb *Nsi*I-*Hpa*I fragment from the 3′ untranslated region) (27); $C_\beta$ (exons 1 to 4; 0.6-kb *Eco*RI insert from the 86T5 cDNA clone); $J_{\beta1}$ (1.6-kb *Bam*HI-*Sac*I fragment encompassing $J_{\beta1.3}$ to $J_{\beta1.7}$); $J_{\beta2}$ (1.2-kb *Eco*RI-*Cla*I fragment encompassing $J_{\beta2.1}$ to $J_{\beta2.7}$); $V_{\beta5.1}$ coding exon (0.2-kb *Eco*RI-*Rsa*I fragment); and $V_{\beta5.1}$ leader and upstream region (0.8-kb *Sac*I-*Xba*I fragment). Riboprobes were generated as instructed by the manufacturer (Promega Corp.) from the Bluescript vector (Stratagene) containing a 0.9-kb *Xba*I-*Eco*RI $C_{\beta1}$ genomic fragment that includes most of IVS1, all of exon 2, IVS2, exon 3, IVS3, and a small portion of exon 4.

PCR was performed on 1 ng of template DNA in a tube containing 2.5 μl of 10× PCR buffer (500 mM KCl, 100 mM Tris [pH 9], 1% Triton X-100), 5 μl of 1 mM deoxynucleoside triphosphates, 2.5 μl of 15 mM $MgCl_2$, 1 μl of oligonucleotide 1 (10 μM), 1 μl of oligonucleotide 2 (10 μM), 11.8 μl of $H_2O$, and 0.2 μl (1 U) of *Taq* DNA polymerase. The DNA was amplified for 30 cycles under the following conditions for each segment: denaturation, 94°C for 0.8 min; annealing, 54°C for 0.8 min; and extension, 72°C for 1.2 min.

The nucleotide sequences of murine IVS2 and $IVS3_{C\beta1}$ were obtained from a 5C.C7 genomic clone (B10.A mouse strain) by dideoxy sequencing methods with Sequenase reagents (U.S. Biochemical Corp.) and have been deposited in GenBank under accession number M97158.

## RESULTS

**Accumulation of intron-containing TCR-β transcripts in the SL12.4 cell clone.** Our previous studies showed that SL12.4 cells possess a fully rearranged TCR-β gene at the β1 locus (Fig. 1A), but mature β1 transcripts are not detectably expressed in the cytoplasm (51). The basis for the lack of mature β1 transcripts was explored in the present investigation. Northern blots containing SL12.4 poly(A)$^+$ RNA were hybridized with a $C_{\beta1}$-specific probe. Figure 1B shows that there was no evidence for mature 1.3-kb $V_\beta C_{\beta1}$ transcripts; instead there was an abundant accumulation of several other $C_{\beta1}$ transcripts. Our subsequent analysis showed that all of these $C_{\beta1}$ transcripts contained introns. For example, an $IVS_{JC\beta1}$ probe hybridized with the two largest TCR-β transcripts of 4.8 and 5.1 kb (Fig. 1B), as expected since $IVS_{JC\beta1}$ is the largest TCR-β intron (Fig. 1A). A detailed analysis of the intron content of each individual $C_{\beta1}$ pre-mRNA is presented below. It should be noted that the terms "pre-mRNA" and "precursor" are used only to designate transcripts that contain introns; these terms are not intended to imply that such transcripts are necessarily capable of being spliced to generate mature transcripts. For example, some intron-containing TCR-β transcripts may be irreversibly modified or sequestered in an environment in which they are incapable of undergoing splicing.

To determine whether all of the $C_{\beta1}$ transcripts that we detected with double-stranded DNA probes are transcribed in the sense orientation, we used sense and antisense single-stranded riboprobes that contained IVS1, IVS2, IVS3, and the intervening exons. The antisense riboprobe hybridized with all major TCR-β transcripts, while a sense riboprobe failed to hybridize with any of the transcripts (data not shown).

The pattern of partially spliced transcripts derived from the β1 locus differed dramatically from transcripts derived from the β2 locus. Our previous studies showed that the SL12.4 cell clone accumulates mature 1.0-kb transcripts that hybridize with a $J_{\beta2}$ probe derived from an unrearranged or partially rearranged β2 gene (51). Here, we used a $C_{\beta2}$-specific probe to confirm that mature 1.0-kb $C_{\beta2}$ transcripts accumulate in SL12.4 cells and also to demonstrate that no

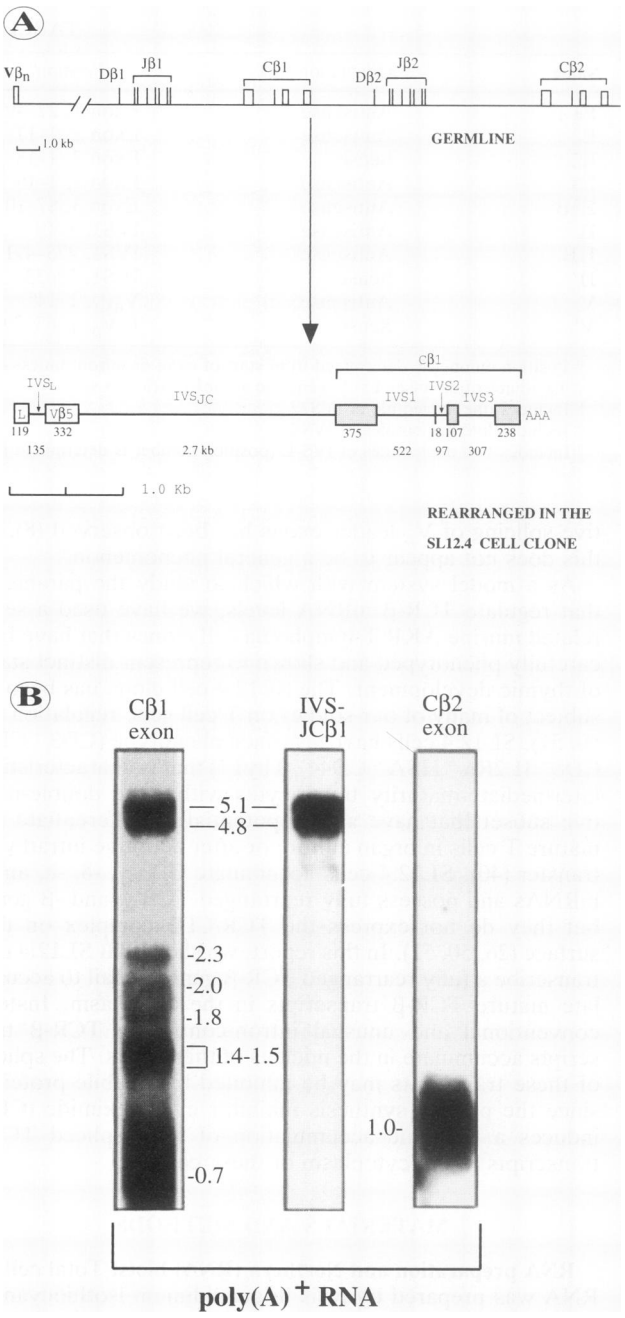


FIG. 1. TCR-β gene rearrangements and expression in the SL12.4 cell clone. (A) The upper portion shows the TCR-β genomic structure (24), and the lower portion provides information on the rearranged β1 gene expressed in SL12.4 cells. Lengths of the exons were derived either from published work (1, 8, 14) or from our sequence analysis of the expressed $V_{\beta5.1}$ element in SL12.4 cells. The lengths of IVS1, IVS2, and IVS3 were also derived from our sequence analysis (Fig. 8 and reference 34). (B) Northern blot analysis of SL12.4 poly(A)$^+$ RNA (1 μg) electrophoresed in a 1% agarose gel. The blot was sequentially hybridized with the probes shown. Sizes are indicated in kilobases.

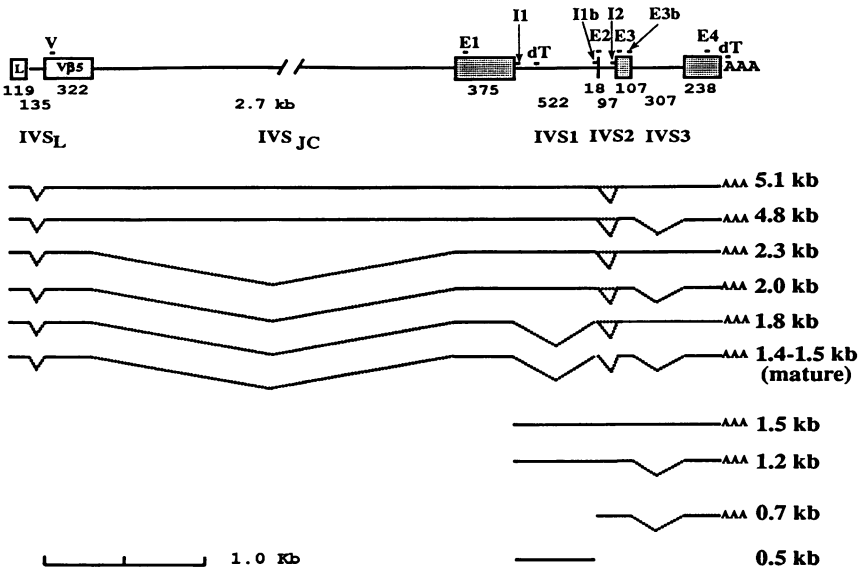


FIG. 2. Schematic diagram of $C_{\beta 1}$ transcripts expressed in SL12.4 cells. Complementary oligonucleotides that bind to SL12.4 TCR-β pre-mRNA at the locations shown were designed (see Table 1 for more information on the oligonucleotides). The splicing pattern and approximate lengths of mapped transcripts were determined by the analysis shown in Fig. 3 and 4. IVS2 was variably present in some transcripts, as indicated by the dotted lines.

$C_{\beta 2}$ pre-mRNAs are evident, even when poly(A)$^+$ RNA was analyzed on Northern blots (Fig. 1B). Thus, SL12.4 cells are capable of efficiently splicing β2 pre-mRNAs but not β1 pre-mRNAs.

**Splicing status of individual TCR-β introns.** By a combination of Northern blot analysis and RNase H mapping, we were able to characterize the β1 RNA splicing products that accumulate in the SL12.4 cell clone. The RNase H mapping protocol involves incubation of RNA with specific oligonucleotides, followed by RNase H cleavage of the RNA at the site where the oligonucleotides bind (RNase H specifically cleaves RNA-DNA hybrids). We chose to use the method of RNase H mapping for several reasons. First, this approach complemented Northern blot analysis, since it allowed more detailed analysis of specific transcripts originally detected by Northern blotting. Second, RNase H mapping permitted us to determine the proportion of transcripts that have spliced out each particular TCR-β intron. Third, RNase H mapping provided information not easily discerned by other methods. It permitted characterization of lariat intermediates. It also allowed characterization of individual transcripts within distinct size classes, while RNase protection analysis is more limited in this regard, particularly if the transcripts are large.

Poly(A)$^+$ RNA from SL12.4 cells was analyzed by RNase H analysis. The expected sizes of the cleavage products were calculated from the known sizes of the TCR-β exons and introns (Fig. 1A). From this analysis, we were able to characterize the splicing status of all of the major $C_{\beta 1}$ transcripts in SL12.4 cells. As discussed below, the cleavage products generated were of sizes consistent with normal splicing intermediates. However, because of space limitations, we do not discuss the origin of all of the major cleavage products generated after RNase H incubation. Figure 2 shows a diagrammatic representation of the intron-containing mRNAs mapped by RNase H analysis. The 1.8-, 2.0-, 2.3-, 4.8-, and 5.1-kb transcripts appear to be conventional splicing intermediates, while the smaller transcripts are unusual products of RNA splicing that will be described below.

**IVS2 and IVS3 splicing.** To investigate the splicing status of IVS3, we used oligonucleotide E3, which binds to a sequence present in exon 3 (Fig. 2). Incubation with this oligonucleotide generated two predominant RNA species of approximately 0.6 and 0.9 kb that hybridized with the $C_{\beta 1}$ exon probe (Fig. 3A, upper panel). The larger 0.9-kb RNA is derived from TCR-β transcripts that have retained IVS3 since this cleavage product also hybridized with the IVS3 probe (Fig. 3A, lower panel). The smear of transcripts below the 0.6- and 0.9-kb species is presumably due to variable lengths of poly(A) tails since RNA cleaved with E3 in the presence of oligo(dT) generated discrete-sized RNA molecules (Fig. 3A, lane 4). These poly(A)$^-$ cleavage products were about 0.3 kb smaller than the predominant poly(A)$^+$ transcripts, indicating that the polyadenylate tail on these TCR-β transcripts is typically 0.3 kb in length. The ratio of the 0.35- and 0.65-kb cleavage products generated after E3 plus dT treatment (determined by densitometric analysis) indicated that approximately 20% of polyadenylated β1 transcripts in SL12.4 cells have retained $IVS3_{C\beta 1}$.

IVS2 and IVS3 RNA splicing was analyzed simultaneously with oligonucleotide E2, which binds to exon 2 (Fig. 2). Cleavage with E2 and dT [oligo(dT) was added to remove polyadenylate tail heterogeneity, as described above] generated three different RNA fragments that hybridized with the $C_{\beta 1}$ exon probe: IVS2$^+$ IVS3$^+$ (0.75- to 0.8-kb), IVS2$^+$ IVS3$^-$ (0.5-kb), and IVS2$^-$ IVS3$^-$ (0.4-kb) cleavage products (Fig. 3B, upper panel). The appropriate products hybridized with IVS2 and IVS3 probes (data not shown). The only potential cleavage product that was not present was an IVS2$^-$ IVS3$^+$ transcript. These results also revealed the proportion of polyadenylated TCR-β transcripts that have spliced IVS2. Comparison of the abundance ratio of the IVS2-containing transcripts (0.5 and 0.75 to 0.8 kb) to IVS2$^-$ transcripts (0.4 kb) indicates that about 50% of the polyadenylated β1 transcripts have retained IVS2.

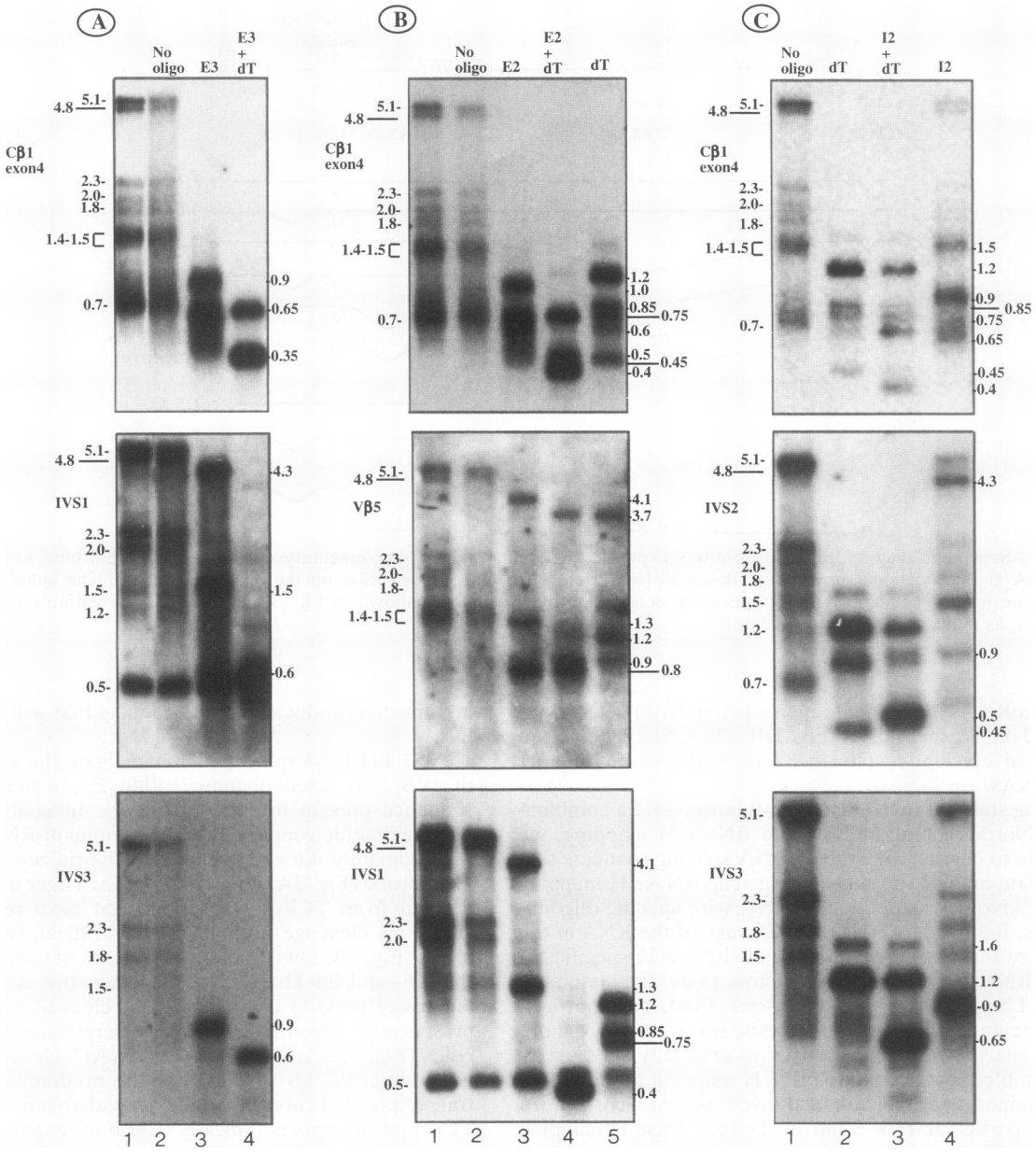


FIG. 3. RNase H analysis of $C_{\beta 1}$ transcripts in SL12.4 polyadenylated RNA. SL12.4 poly(A)$^+$ RNA (1 μg) was subjected to RNase H analysis using the oligonucleotides shown, followed by electrophoresis in 1% agarose gels and Northern blot hybridization. Each panel shows the results with a single blot sequentially hybridized with the probes shown. Lanes marked "No oligo" refers to RNA subjected to the RNase H procedure in the absence of a specific oligonucleotide; unmarked lanes show untreated RNAs used as controls. Sizes are indicated in kilobases.

The splicing status of IVS2 was confirmed by use of oligonucleotide I2, which binds to the 3′ end of IVS2 (Fig. 2). Cleavage with I2 sharply reduced the levels of the 1.8-, 2.0-, 2.3-, 4.8-, and 5.1-kb β1 transcripts (Fig. 3C, upper panel). Therefore, a proportion of these transcripts must contain this small intron (97 nucleotides), as indicated by the diagram in Fig. 2. However, since some uncleaved transcripts persist (even after incubation with a 10-fold-higher concentration of I2; data not shown), some of these transcripts must have spliced out IVS2.

**IVS1 and $IVS_{JC}$ splicing.** The splicing status of IVS1 and $IVS_{JC}$ was analyzed by cleavage with oligonucleotide E2 and hybridization with a $V_\beta$ probe to assess the 5′ cleavage products that could potentially contain these introns (Fig. 2). The particular $V_\beta$ element rearranged to the $C_{\beta 1}$ locus in SL12.4 cells was determined by hybridization of $^{32}$P-labeled SL12.4 total cDNA to cold $V_\beta$ probes immobilized on membranes. This analysis revealed that SL12.4 cells expressed a member of the $V_{\beta 5}$ family. Sequence analysis (to be described elsewhere) confirmed this result and in particular showed that the SL12.4 cell clone transcribed the $V_{\beta 5.1}$ gene segment. Figure 3B (middle panel) shows that a $V_{\beta 5}$ probe hybridized with the 1.8-, 2.0-, 2.3-, 4.8-, and 5.1-kb precursor transcripts, as expected. Incubation with E2 gen-

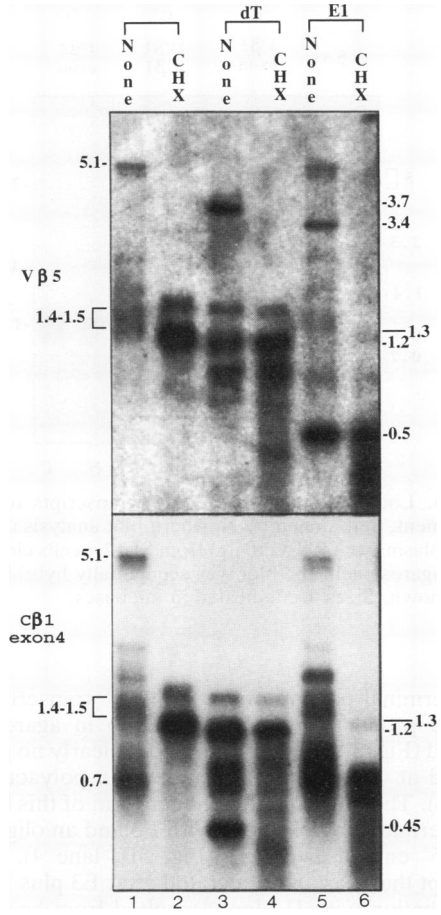


FIG. 4. RNase H analysis: effect of CHX on SL12.4 $C_{\beta 1}$ transcripts. SL12.4 poly(A)$^+$ RNA (0.2 μg of RNA from CHX-treated cells [10 μg/ml for 6 h] and 1 μg of RNA from control cells [labeled "None"]) was subjected to the analysis described in the legend to Fig. 3. The first two lanes show RNA incubated under the same conditions as the others but without a specific oligonucleotide. Sizes are indicated in kilobases.

erated three dominant $V_{\beta 5}{}^+$ cleavage products with the expected sizes: 0.8 kb ($IVS_{JC}{}^-$ $IVS1^-$), 1.3 kb ($IVS_{JC}{}^-$ $IVS1^+$), and 4.1 kb ($IVS_{JC}{}^+$ $IVS1^+$). Hybridization with an IVS1 probe confirmed these identities. The proportion of polyadenylated transcripts that excised IVS1 was determined by calculating the ratio of $IVS1^+$ (1.3- and 4.1-kb) and $IVS1^-$ (0.8-kb) transcripts generated after E2 treatment. This analysis revealed that about 50% of polyadenylated β1 transcripts contained IVS1 sequences.

Further confirmation that many β1 transcripts possess IVS1 was shown by cleavage with oligo(dT). This oligonucleotide cleaves near the 5′ end of IVS1 because of the presence of several tracts of adenylate residues that span the region between nucleotides 100 to 155 of $IVS1_{C\beta 1}$, including a homogeneous poly(A) tract of 22 nucleotides (34). Incubation with dT cleaved $IVS1^+$ transcripts to the expected sizes, as assessed with the IVS1, $V_{\beta 5}$, and $C_{\beta 1}$ exon probes (Fig. 3B and C). Note that the IVS1 probe recognized only the 3′ products that result from dT cleavage.

The splicing status of $IVS_{JC}$ was further assessed with oligonucleotide E1, which binds to sequences in exon 1 (Fig. 2). Oligonucleotide E1 generated 0.5- and 3.4-kb cleavage products that hybridized with the $V_{\beta 5}$ probe that correspond to $IVS_{JC}{}^-$ and $IVS_{JC}{}^+$ transcripts, respectively (Fig. 4, lane 5). The ratio of these two products shows that only about 10% of polyadenylated β1 transcripts have retained the JC intron.

**$IVS_L$ splicing.** The splicing status of the most 5′ intron, $IVS_L$, was also assessed with oligonucleotide E1. The size of the $IVS_{JC}{}^-$ cleavage product (0.5 kb) generated after E1 cleavage (Fig. 4) is consistent with an RNA that has already spliced out $IVS_L$. No cleavage product that contained the 135-nucleotide $IVS_L$ (this product would be 0.6 to 0.7 kb) was detected. Further evidence that $IVS_L$ is spliced out of virtually all β1 transcripts included the following. First, RNase H cleavage in the presence of an oligonucleotide complementary with the $V_{\beta 5}$ coding segment (oligonucleotide V; Fig. 2) generated only a 0.1-kb (spliced) product recognized by a $V_{\beta 5}$ leader probe (data not shown). Second, an $IVS_L$ probe failed to hybridize detectably with any of the major β1 transcripts (data not shown).

**IVS2 5′ cleavage intermediate.** RNase H mapping showed that the abundant 0.7-kb transcript detected with the $C_{\beta 1}$ and IVS2 probes (Fig. 3C, lane 1) is a novel splicing intermediate containing IVS2 at the 5′ terminus (Fig. 2). The evidence for this is as follows. Oligo(dT) treatment reduced the size of the 0.7-kb transcript to 0.45 to 0.5 kb (Fig. 3C, upper panel), showing that it possessed a 0.45- to 0.5-kb deadenylated body and a 0.2- to 0.25-kb poly(A) tail. This size is consistent with a transcript that has spliced out IVS3 and possesses IVS2 at its 5′ terminus. This phenotype was confirmed by the following results. First, the IVS2 probe hybridized with the 0.45- to 0.5-kb cleavage product generated after dT treatment (Fig. 3C, middle panel). Second, the IVS3 probe did not hybridize with this 0.45- to 0.5-kb cleavage product (Fig. 3C, lower panel). Third, I2 plus dT treatment generated a product 0.1 kb smaller (approximately 0.4 kb) than the product generated by treatment with dT alone; this cleavage product did not hybridize with the IVS2 probe (Fig. 3C), as expected since I2 incubation should remove IVS2 from the 5′ end of this transcript. Fourth, when the 0.7-kb transcript was gel purified prior to RNase H analysis, it displayed the appropriate size and hybridization characteristics when cleaved in the presence of the oligonucleotide I2, E3, or E4 (data not shown).

To determine more precisely the 5′ terminus of the 0.7-kb transcript, poly(A)$^+$ RNA was cleaved with an oligonucleotide complementary to the 3′ end of exon 3, E3b, and then subjected to polyacrylamide gel electrophoresis, followed by electroblotting and filter hybridization with an IVS2 probe. The 0.18-kb E3b cleavage product derived from the 0.7-kb transcript nearly comigrated with the cleavage product generated after incubation with E3b plus E2 (Fig. 5A), indicating that the 0.7-kb transcript possesses IVS2 at its 5′ terminus (see Fig. 2 and Table 1 for positions of the oligonucleotides). The 5′ terminus of the 0.7-kb transcript did not include exon 2 since the E3b cleavage product (0.18 kb) was clearly smaller than the 0.20-kb exon 2-containing cleavage product generated from the conventional TCR-β splicing intermediates after E3b plus I1b incubation (Fig. 5A). It is unlikely that IVS2 at the terminus of the 0.7-kb transcript is in a lariat conformation since the 0.18-kb E3b cleavage product derived from this transcript did not displayreduced migration in the polyacrylamide gel, as is typical for intron lariats (32, 52), including $IVS1_{C\beta 1}$ (34). In fact, the 0.18-kb E3b cleavage product derived from the 0.7-kb transcript migrated slightly faster than the E3b plus E2 cleavage product (Fig. 5A), indicating that it is likely that IVS2 has been debranched and

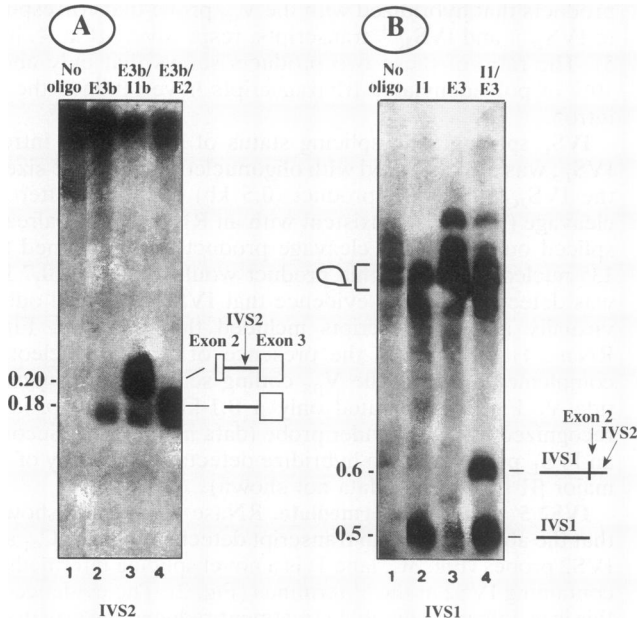


FIG. 5. Characterization of $C_{\beta 1}$ transcripts that possess introns at the 5′ end. (A) SL12.4 poly(A)$^+$ RNA (1 μg) was subjected to RNase H analysis using the oligonucleotides shown, followed by electrophoresis in a 7% denaturing polyacrylamide gel and Northern blot hybridization with a $IVS2_{C\beta 1}$ probe. Lane 1 represents RNA subjected to the RNase H procedure in the absence of a specific oligonucleotide. (B) The same conditions as for panel A except that a 5% polyacrylamide gel was used and the hybridization probe was $IVS1_{C\beta 1}$. Sizes are indicated in kilobases.

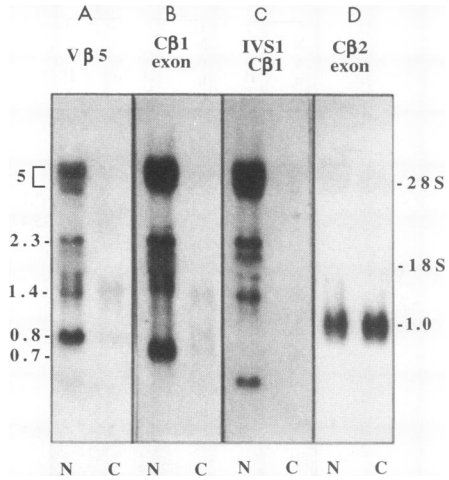


FIG. 6. Localization of SL12.4 $C_{\beta 1}$ transcripts to the nuclear compartment, determined by Northern blot analysis of nuclear (N) and cytoplasmic (C) RNA (10 μg) from SL12.4 cells electrophoresed in a 1% agarose gel. The blot was sequentially hybridized with the probes shown. Sizes are indicated in kilobases.

nibbled at the 5′ end. We conclude that the abundant 0.7-kb β1 transcript is an IVS2$^+$ IVS3$^-$ linear RNA molecule that appears to have undergone the first step of IVS2 splicing in vivo (5′ cleavage) but has not been subjected to the second step (3′ cleavage) which would have lead to expulsion of IVS2 and joining of exons 2 and 3.

**IVS1 5′ cleavage intermediates.** The 1.2- and 1.5-kb IVS1$^+$ transcripts appear to be splicing intermediates that contain IVS1 at the 5′ terminus (Fig. 2) and differ only in that the former transcript has spliced out IVS3 (Fig. 3A). Evidence for the existence of transcripts that possess IVS1 at the 5′ end is as follows. RNase H cleavage in the presence of E3 released a 0.6-kb cleavage product that hybridized with IVS1 and IVS2 probes (Fig. 3A, middle panel, and data not shown). The size and hybridization characteristics of this 0.6-kb product indicated that it contains IVS2 and that its 5′ terminus is the 5′ end of IVS1. Intron IVS1 at the 5′ termini of the 1.2- and 1.5-kb transcripts appears to be in a lariat conformation. Electrophoresis of the RNA in a 5% polyacrylamide gel, followed by electroblotting and filter hybridization with an IVS1 probe, did not reveal any transcripts that migrated at 1.2 or 1.5 kb, which would be expected if they were linear molecules. Under these conditions, the only major transcripts detected were two RNA species (Fig. 5B, lane 1) which we show elsewhere (34) are free (exonless) 0.5-kb IVS1 lariats with different-length tails (in contrast to their slow migration in polyacrylamide gels, these free intron lariat molecules migrate as a single 0.5-kb transcript in agarose gels [34]).

To provide further evidence that transcripts with IVS1 at the 5′ terminus are lariats, SL12.4 poly(A)$^+$ RNA was incubated with oligonucleotide E3 and RNase H to release the 5′-terminal portion of these IVS1$^+$ transcripts. The E3 cleavage product migrated as 0.6 kb in agarose gels, as expected (Fig. 3A, middle panel), but clearly no product that migrated at 0.6 kb was detectable in a polyacrylamide gel (Fig. 5B). The migration of a linear form of this 0.6-kb RNA was determined by cleavage with E3 and an oligonucleotide to the 5′ end of IVS1, I1 (Fig. 5B, lane 4). The 0.5-kb transcript that was also generated after E3 plus I1 treatment (or incubation with I1 alone) resulted from linearization of the free IVS1 lariat (34). It was not feasible to independently analyze whether these splicing intermediates are in a lariat conformation by using debranching extracts (HeLa S100 or nuclear extracts) because such extracts only very inefficiently debranch IVS1, perhaps for the same reason that this intron is not efficiently debranched in vivo (34).

**Accumulation of TCR-β pre-mRNAs in the nucleus of the SL12.4 cell clone.** One possible mechanism to prevent the splicing of β1 transcripts would be to export partially spliced transcripts to the cytoplasm where RNA splicing does not occur. Retroviruses employ this export mechanism to generate an array of unspliced, partially spliced, and fully spliced transcripts in the cytoplasm that give rise to different translation products. We found that such an export mechanism is unlikely to be operating on β1 pre-mRNAs since these transcripts were clearly confined to the nuclear compartment (Fig. 6A to C). By comparison, the fully spliced 1.0-kb β2 transcript was present in both the nuclear and cytoplasmic compartments (Fig. 6D). Most of the β1 transcripts present in nuclear RNA, including the abundant 0.7-kb transcripts possessing IVS2 at the 5′ terminus (Fig. 6), were also present in poly(A)$^+$ RNA (Fig. 1B and 3). This result shows that the polyadenylation of many β1 transcripts precedes initial RNA splicing events.

A unique nuclear transcript not present in poly(A)$^+$ RNA was an abundant 0.8-kb $V_{\beta 5}{}^+$ transcript (Fig. 6A). The size and hybridization characteristics of this transcript suggest that it is the 5′ portion of precursor transcripts that have undergone 5′ cleavage of IVS1 or IVS2 but have failed to undergo 3′ cleavage and exon ligation (see above). Such a 5′ cleavage product would not contain a polyadenylated tail

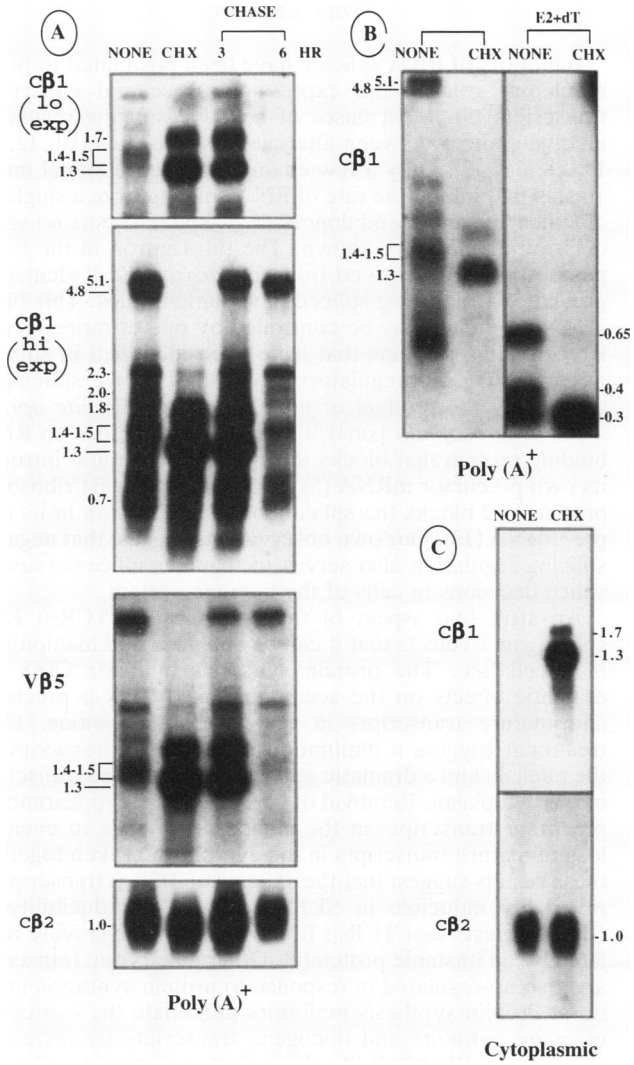


FIG. 7. Reversible effects of CHX on TCR-β mRNA accumulation. (A) Northern blot analysis of SL12.4 poly(A)$^+$ RNA (1 μg) from control cells (none), cells incubated for 12 h with 10 μg of CHX per ml (CHX), or cells treated with CHX and then washed and recultured for 3 or 6 h (chase). The RNA was electrophoresed in a 1% agarose gel, blotted, and sequentially hybridized with the probes shown. Equivalent amounts of RNA were loaded in each lane as assessed by methylene blue staining (49) except the last lane, which had approximately one-half as much RNA as did the other lanes. (B) SL12.4 poly(A)$^+$ RNA (0.5 μg of RNA from CHX-treated cells [10 μg/ml for 6 h] and 1 μg of RNA from control cells [labeled "none"]) was subjected to RNase H analysis in the absence of oligonucleotides (first two lanes) or the presence of the oligonucleotides E2 and oligo(dT) (last two lanes). The RNA was electrophoresed in 1% agarose gels, blotted, and hybridized with the probe shown. (C) Northern blot analysis of cytoplasmic RNA (10 μg) from SL12.4 cells, performed as described for panel A. Sizes are indicated in kilobases.

and thus would not be expected to be in the poly(A)$^+$ fraction.

**The protein synthesis inhibitor CHX allows mature TCR-β transcripts to accumulate in the cytoplasm.** The accumulation of partially spliced β1 transcripts in SL12.4 cells shows that the splicing of β1 transcripts is impaired in this cell clone. We previously showed that CHX induces the appearance of a fully spliced 1.3-kb TCR-β transcript that hybridizes with a $J_{\beta1}$ probe. We concluded that this induction of mature TCR-β mRNA was a posttranscriptional event since it occurred without a significant concomitant increase in the rate of transcription, as judged by nuclear runoff assays (51). It was hypothesized that an unstable inhibitor protein blocks the expression of mature TCR-β transcripts by a posttranscriptional mechanism. If the putative inhibitor acts by inhibiting RNA splicing, it would be anticipated that if the inhibitor was depleted (by addition of CHX), precursor transcripts would be depressed in levels. Figure 7A shows that, indeed, CHX treatment led to the down-regulation of $V_{\beta5}C_{\beta1}$ pre-mRNAs and the dramatic appearance of a 1.3-kb fully spliced $V_{\beta5}C_{\beta1}$ mRNA. A novel 1.7-kb $V_{\beta5}C_{\beta1}$ transcript was also induced by CHX; this transcript is a mature cytoplasmic mRNA that is derived from a promoter upstream of the transcription initiation site for 1.3-kb transcripts (unpublished observations). Confirmation that CHX induced a fully spliced β1 transcript came from RNase H analysis. IVS2 and IVS3 were fully spliced following CHX treatment, as evidenced by a single 0.3-kb cleavage product recognized by the $C_{\beta1}$ exon probe after oligonucleotide E2 plus dT cleavage (Fig. 7B, right panel).

The mature TCR-β transcripts induced by CHX were exported to the cytoplasm (Fig. 7C, right lane). Virtually no β1 transcripts were in the cytoplasm before treatment (Fig. 7C, left lane). In contrast, 1.0-kb β2 transcripts were present in the cytoplasm before and after CHX treatment (Fig. 7C). Removal of CHX led to the rapid reappearance of intron-containing $V_{\beta5}C_{\beta1}$ transcripts and the disappearance of the major mature 1.3-kb $V_{\beta5}C_{\beta1}$ transcript (Fig. 7A). The reciprocal expression pattern of intron-containing and mature β1 transcripts in response to CHX suggests that there is a precursor-product relationship between these two classes of transcripts. This notion is substantiated by our observation that treatment of SL12.4 cells with the transcriptional inhibitor actinomycin D does not prevent the induction of mature β1 mRNA in response to CHX (unpublished observations). Taken together, the data indicate that CHX is likely to act, at least in part, by increasing the rate of TCR-β RNA splicing.

**Fully spliced TCR-β transcripts accumulate in the nuclei of SL12.4 cells.** If inhibited RNA splicing were the only mechanism that prevented TCR-β mRNA accumulation in the cytoplasm of SL12.4 cells, then fully spliced TCR-β transcripts should also be absent in the nucleus. Since we showed that none of the TCR-β introns are completely blocked in splicing, it would not be surprising if some fully spliced TCR-β transcripts were generated in SL12.4 cells. Northern blot analysis indicated that fully spliced 1.4- to 1.5-kb TCR-β transcripts with long poly(A) tails that varied somewhat in size were detectable with both $V_{\beta5}$ and $C_{\beta1}$ exon probes (Fig. 7A). Cleavage with oligo(dT) and RNase H showed that the deadenylated body of these 1.4- to 1.5-kb transcripts from untreated SL12.4 cells migrated identically (1.2 kb) to the deadenylated body of the CHX-induced 1.3-kb transcript (Fig. 4; note that five times more RNA from untreated cells than from CHX-treated cells was loaded). Thus, at least a proportion of the 1.4- to 1.5-kb transcripts in untreated SL12.4 cells are fully spliced TCR-β mRNAs present in the nucleus that have longer poly(A) tails than do the 1.3-kb mature transcripts induced by CHX to appear in the cytoplasm. This observation is consistent with other studies demonstrating that nuclear mRNAs possess longer poly(A) tails than do cytoplasmic mRNAs (6). It should be noted that this analysis provides an overestimate of the relative abundance of fully spliced messages since the anal-

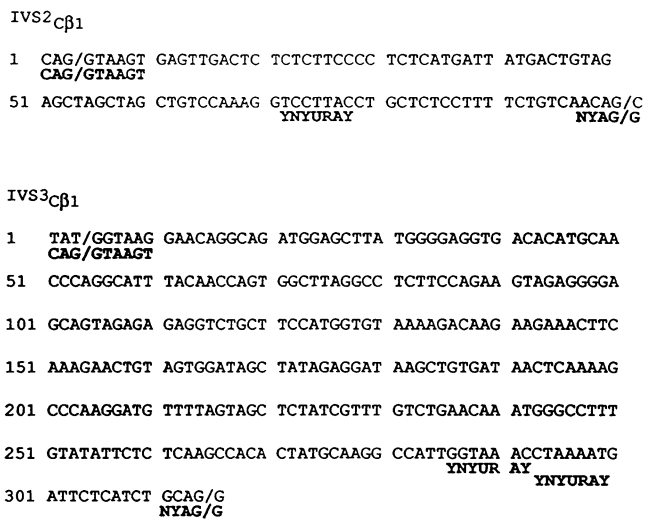


FIG. 8. Nucleotide sequences of $IVS2_{C\beta1}$ and $IVS3_{C\beta1}$. The sequences shown in bold below the $C_{\beta1}$ intron sequence represent the consensus sequences for mammalian branchpoint regions (53) and 5′/3′ splice junctions (30). The sequence shown is in agreement with a partial sequence of murine $IVS2_{C\beta1}$ and $IVS3_{C\beta1}$ reported previously (14).

ysis was conducted on the poly(A)$^+$ fraction of RNA which lacks many TCR-β pre-mRNAs, particularly those containing $IVS_{JC\beta1}$ (see above). We conclude that although $C_{\beta1}$ transcripts display inhibited splicing in SL12.4 cells, the presence of some fully spliced $C_{\beta1}$ transcripts in the nucleus implies that some other posttranscriptional mechanism(s) must also contribute to the lack of mature transcripts in the cytoplasm.

**Sequence of $C_{\beta1}$ introns.** The sequences of the $C_{\beta1}$ introns were determined since they displayed unusual splicing behavior. The sequence of $IVS1_{C\beta1}$ is presented elsewhere (34); our analysis revealed that it possesses canonical splicing signals. The complete sequences of $IVS2_{C\beta1}$ and $IVS3_{C\beta1}$ are shown in Fig. 8. Both introns possess the invariant GU and AG (30) at their 5′ and 3′ ends, respectively. $IVS2_{C\beta1}$ has many other features expected of a typical intron. First, it has a 5′ splice junction region that displays perfect complementarity with the portion of U1 known to interact with this region (30). Second, it has a stretch of 17 of 19 polypyrimidines ($Y_n$) followed by the sequence AACAG/C which has some similarity with the known consensus 3′ splice junction, $Y_n$NYAG/G (30). Third, just upstream of the polypyrimidine tract, it possesses a sequence displaying a six-of-seven match with the mammalian branchpoint consensus sequence, YNYURAY (53). Thus, the inhibited splicing of $IVS2_{C\beta1}$ cannot be easily ascribed to inefficient splicing signals. $IVS3_{C\beta1}$, which was more efficiently spliced than IVS2 in SL12.4 cells, has features less consistent with a typical intron. Most strikingly, it has a stretch of only 9 of 12 polypyrimidine residues upstream of its splice acceptor (Fig. 8). Studies of other introns have indicated that short polypyrimidine tracts typically do not permit efficient splicing (41). However, $IVS3_{C\beta1}$ does have a consensus 3′ splice junction ($Y_n$GCAG/G) and two potential branchpoint sequences upstream of the short polypyrimidine tract, each of which displays a five-of-seven match with the known consensus sequence. The 5′ splice site of IVS3 possesses six of nine nucleotides in common with the known consensus sequence (30).

## DISCUSSION

Inhibitors of RNA splicing have been postulated to play a regulatory role in the expression of several eukaryotic transcripts (5). Most cases of negative splicing regulation involve choices between alternative splice sites (10, 12, 15, 19, 28, 36, 43). Only a few examples of repressional mechanisms that inhibit the rate of RNA splicing from a single set of splice acceptors and donors (e.g., splice-versus-no-splice decision making) are known. The third intron in the transposase transcript derived from the *Drosophila* P element is prevented from being spliced in somatic tissues. This block in RNA splicing may be controlled by one or more specific RNA-binding proteins that have been identified in somatic tissues (46). Autoregulatory control of RNA splicing is exerted by the product of the suppressor of *white apricot* locus of *Drosophila* [*su*($W^a$)]. This locus encodes an RNA-binding protein that blocks the splicing of the first intron of its own precursor mRNA (5). Similarly, the yeast ribosomal protein L32 blocks the splicing of a single intron in its own pre-mRNA (13). Our own observations suggest that negative splicing regulation also serves to regulate splice-versus-no-splice decisions in cells of the immune system.

An attractive aspect of the regulation of TCR-β RNA splicing in T cells is that it can be analyzed and manipulated in a cell line. The protein synthesis inhibitor CHX has dramatic effects on the accumulation of TCR-β precursor and mature transcripts in the SL12.4 cell clone. CHX treatment triggers a diminution of precursor transcripts in the nucleus and a dramatic appearance of spliced transcripts in the cytoplasm. Removal of CHX permits reappearance of precursor transcripts in the nucleus and leads to eventual loss of mature transcripts in the cytoplasm. Taken together, these results suggest that the splicing of TCR-β transcripts is reversibly inducible in SL12.4 cells. The inducibility by CHX suggests that TCR-β RNA splicing is negatively regulated by an unstable protein(s). Other eukaryotic transcripts are also up-regulated in response to protein synthesis inhibitors. Protein synthesis inhibitors potentiate the expression of many cytokine and oncogene transcripts by increasing cytoplasmic RNA half-life. The effect is mediated, at least in part, by an AU-rich sequence present in the 3′ untranslated region (39) which binds to a specific protein that may play a role in the stability of these messages (7). Protein synthesis inhibitors also induce immunoglobulin κ chain gene transcription (47), perhaps as a result of depleting cells of I-κB, an inhibitor of the positive transcription factor NF-κB (3).

Thus, protein synthesis inhibitors have been useful tools to provide evidence for negative regulatory mechanisms that act at the level of gene transcription or cytoplasmic RNA stability. The effect of protein synthesis inhibitors on TCR-β expression is unusual since it does not appreciably affect TCR-β gene transcription (51) but instead appears to have a profound effect on TCR-β RNA splicing. This characteristic provides a unique system with which to study the mechanism of RNA splicing. It should be stressed, however, that it is not clear that CHX is acting by depleting T cells of a specific inhibitor of RNA splicing. Since the synthesis of most cellular proteins is blocked by CHX, other, less specific events may be responsible for its effects on RNA splicing. Nevertheless, the dramatic effects of CHX on TCR-β transcripts suggest that it will be a useful tool with which to investigate the regulation of TCR-β RNA splicing.

Several factors must be taken into account when one is considering the mechanism that controls TCR-β RNA splicing in SL12.4 cells. First, the splicing of several introns is

impaired. Second, only the most 5′ intron within a $V_\beta$-containing transcript, $IVS_L$, is efficiently spliced. Third, the individual introns display different apparent rates of splicing. We assessed the percentage of polyadenylated transcripts that contained each intron as an indirect measure of the splicing rate in vivo. $IVS1_{C\beta1}$ and $IVS2_{C\beta1}$ are retained in about one-half of β1 transcripts, while $IVS3_{C\beta1}$ is present in only about 1/10 of β1 transcripts. $IVS_{JC\beta1}$ is present in only about 1/10 of polyadenylated β1 transcripts, although it is clearly present in a larger proportion of total nuclear β1 transcripts, as detected by Northern blot analysis (Fig. 6).

One model to explain the pattern of TCR-β RNA splicing that we observe is to hypothesize that unstable regulatory proteins independently regulate each of the four introns that display inhibited splicing. Another model is that, instead, only one or a few introns are directly inhibited from undergoing splicing by regulatory proteins. The other introns would display inefficient splicing as a consequence of the regulatory introns. This transfer of inhibitory activity could be mediated by interactions between the introns, as has been noted for other transcripts (31, 45). Our data are consistent with a model in which negative regulation is focused on $IVS1_{C\beta1}$ and $IVS2_{C\beta1}$. There are three lines of evidence that support this specific model. First, IVS1 and IVS2 are present in a greater proportion of pre-mRNAs than is IVS3 or $IVS_{JC}$. Second, the particular combination of introns that are present in TCR-β pre-mRNAs suggests that the splicing of IVS1 and IVS2 is less efficient than the splicing of $IVS_{JC}$ and IVS3, respectively. Third, 3′ splice site cleavage is inefficient or repressed for IVS1 and IVS2 but not the other introns. The evidence for this notion is the accumulation of splicing intermediates that have cleaved the 5′ splice site but not the 3′ splice site of these two introns.

The accumulation of splicing intermediates in vivo that have undergone 5′ splice cleavage but not cleavage of the 3′ splice site is a novel observation. Other eukaryotic pre-mRNAs have been commonly shown to generate splicing intermediates of this type during in vitro splicing reactions (22, 32), but such intermediates are rarely observed at detectable levels in vivo (52). Presumably, such 5′ splicing intermediates accumulate during in vitro splicing reactions because splicing is inefficient in vitro, while in vivo splicing reactions typically display such a rapid kinetic linkage of the first and second steps of splicing that intermediates are not normally detectable. The 5′ splice site cleavage intermediates that have been observed in vitro and in vivo by other workers accumulate as lariat structures (22, 32, 52). Similarly, TCR-β splicing intermediates which contain $IVS1_{C\beta1}$ at the 5′ termini are in a lariat conformation (Fig. 5B), just as we previously showed for free $IVS1_{C\beta1}$ (34). In contrast, the extremely abundant 0.7-kb splicing intermediate which contains $IVS2_{C\beta1}$ at the 5′ terminus is likely to be linear, as judged from migration in polyacrylamide gels. This observation suggests that the IVS2 lariat structure has been debranched in vivo. This debranched transcript may have lost its ability to undergo 3′ cleavage and exon ligation. Thus, this unusual transcript may be on a dead-end pathway. However, we cannot rule out an alternative possibility that this linear transcript was generated not by the classical splicing reaction but instead by specific endonucleolytic cleavage.

What is the function of this negative posttranscriptional regulation that acts, in part, at the level of RNA splicing? (D)$JC_\beta$, CD3-γ, -δ, -ε, and -ζ, CD4, and CD8-α transcripts do not display impaired splicing (50; this study), so the regulation appears to be a selective mechanism that acts on V(D)$JC_\beta$ transcripts. One possibility is that a specific RNA splicing mechanism controls the stage specific accumulation of mature cytoplasmic V(D)$JC_\beta$ transcripts during thymic maturation. Consistent with this hypothesis is our observation that TCR-β splicing intermediates accumulate in normal thymocytes (34). These thymic splicing intermediates correspond in intron content to those which accumulate in the SL12.4 cell clone described in this report (unpublished observations). The rate of RNA splicing may serve to control the expression of TCR-β protein in a developmentally regulated fashion, in combination with other regulated events such as gene rearrangements.

## ACKNOWLEDGMENTS

We are grateful to the following individuals for providing cloned TCR-β DNA: S. Hedrick (UCSD, San Diego, Calif.) for a cloned $C_{\beta1}$ genomic DNA fragment (5C.C7) and the 86T5 cDNA clone, E. Palmer (National Jewish Center, Denver, Colo.) for the $C_{\beta1}$ 3′ untranslated region and a complete set of subcloned $V_\beta$ fragments, D. Loh (Washington University, St. Louis, Mo.) for $V_{\beta5}$ genomic clones, and M. Blackman, P. Marrack, and J. Kappler (National Jewish Center) for a cloned $C_{\beta2}$ genomic DNA fragment (a $V_{\beta8.1}D_{\beta2}J_{\beta2.3}C_{\beta2}$ construct).

This work was supported by NIH grant GM39586.

## REFERENCES

1. **Anderson, S. J., H. S. Chou, and D. Y. Loh.** 1988. A conserved sequence in the T-cell receptor β-chain promoter region. Proc. Natl. Acad. Sci. USA **85**:3551–3554.
2. **Ashwell, J. D., and R. D. Klausner.** 1990. Genetic and mutational analysis of the T-cell antigen receptor. Annu. Rev. Immunol. **8**:139–167.
3. **Baeuerle, P. A., and D. Baltimore.** 1988. IκB: a specific inhibitor of the NF-κB transcription factor. Science **242**:540–546.
4. **Behlke, M. A., and D. Y. Loh.** 1986. Alternative splicing of murine T-cell receptor β-chain transcripts. Nature (London) **322**:379–382.
5. **Bingham, P. M., T. Chou, I. Mims, and Z. Zachar.** 1988. On/off regulation of gene expression at the level of splicing. Trends Biochem. Sci. **4**:134–138.
6. **Brawerman, G.** 1975. Metabolism of the polyadenylate sequence of nuclear RNA and messenger RNA in mammalian cells. Cell **5**:271–280.
7. **Brewer, G.** 1991. An A+U-rich element RNA-binding factor regulates c-*myc* mRNA stability in vitro. Mol. Cell. Biol. **11**:2460–2466.
8. **Chou, H. S., S. J. Anderson, M. C. Louie, S. A. Godambe, M. R. Pozzi, M. A. Behlke, K. Huppi, and D. Loh.** 1987. Tandem linkage and unusual RNA splicing of the T-cell receptor β-chain variable-region genes. Proc. Natl. Acad. Sci. USA **84**:1992–1996.
9. **Dent, A. L., P. J. Fink, and S. M. Hedrick.** 1989. Characterization of an alternative exon of the murine T cell receptor β-chain. J. Immunol. **143**:322–328.
10. **D'Orval, B. C., Y. D. Carafa, P. Sirand-Pugnet, M. Gallego, E. Brody, and J. Marie.** 1991. RNA secondary structure repression of a muscle-specific exon in HeLa cell nuclear extracts. Science **252**:1823–1828.
11. **Doskow, J., and M. F. Wilkinson.** 1992. CD3-γ, -δ, -ε, -ζ, TCR-α and -β transcripts are independently regulated during thymocyte ontogeny and T cell activation. Immunology **77**:465–468.
12. **Emeson, R. B., F. Hedjran, J. M. Yeakley, J. W. Guise, and M. G. Rosenfeld.** 1989. Alternative production of calcitonin and CGRP mRNA is regulated at the calcitonin-specific splice acceptor. Nature (London) **341**:76–80.
13. **Eng, F. J., and J. R. Warner.** 1991. Structural basis for the regulation of splicing of a yeast messenger RNA. Cell **65**:797–804.
14. **Gascoigne, N. R. J., Y. Chien, D. M. Becker, J. Kavaler, and M. M. Davis.** 1984. Genomic organization and sequence of T-cell receptor β-chain constant- and joining-region genes.

Nature (London) **310:**387–391.
15. **Gattoni, R., K. Chebli, M. Himmelspach, and J. Stevenin.** 1991. Modulation of alternative splicing of adenoviral E1A transcripts: factors involved in the early-to-late transition. Genes Dev. **5:**1847–1858.
16. **Haars, R., M. Kronenberg, W. M. Gallatin, I. L. Weissman, F. L. Owen, and L. Hood.** 1986. Rearrangement and expression of T cell antigen receptor and γ genes during thymic development. J. Exp. Med. **164:**1–24.
17. **Hashimoto, Y., A. M. Maxam, and M. I. Greene.** 1990. Identification of tissue specific nuclear proteins: DNA sequence and protein binding regions in the T cell receptor β J-C intron. Nucleic Acids Res. **18:**3027–3037.
18. **Herman, A., J. W. Kappler, P. Marrack, and A. M. Pullen.** 1991. Superantigens: mechanism of T-cell stimulation and role in immune responses. Annu. Rev. Immunol. **9:**745–772.
19. **Inoue, K., K. Hoshijima, H. Sakamoto, and Y. Shimura.** 1990. Binding of the Drosophila Sex-lethal gene product to the alternative splice site of the transformer primary transcript. Nature (London) **344:**461–463.
20. **Jamieson, C., F. Mauxion, and R. Sen.** 1989. Identification of a functional NF-κB binding site in the murine T cell receptor β2 locus. J. Exp. Med. **170:**1737–1743.
21. **Kishi, H., P. Borgulya, B. Scott, K. Karjalainen, A. Traunecker, J. Kaufman, and H. von Boehmer.** 1991. Surface expression of the β T cell receptor (TCR) chain in the absence of other TCR or CD3 proteins on immature T cells. EMBO J. **10:**93–100.
22. **Krainer, A. R., T. Maniatis, B. Ruskin, and M. R. Green.** 1984. Normal and mutant human β-globin pre-mRNAs are faithfully and efficiently spliced in vitro. Cell **36:**993–1005.
23. **Krimpenfort, P., R. de Jong, Y. Uematsu, Z. Dembic, S. Ryser, H. von Boehmer, M. Steinmetz, and A. Berns.** 1988. Transcription of T cell receptor β-chain genes is controlled by a downstream regulatory element. EMBO J. **7:**745–750.
24. **Kronenberg, M., G. Siu, L. E. Hood, and N. Shastri.** 1986. The molecular genetics of the T-cell antigen receptor and T-cell antigen recognition. Annu. Rev. Immunol. **4:**529–591.
25. **Lanier, E. R., R. M. Brown, and E. Kraig.** 1991. Binding of thymic factors to the conserved decanucleotide promoter element of the T-cell receptor $V_\beta$ gene is developmentally regulated and is absent in SCID mice. Proc. Natl. Acad. Sci. USA **88:**8131–8135.
26. **MacLeod, C. L., L. Minning, D. P. Gold, C. Terhorst, and M. F. Wilkinson.** 1986. Negative trans-regulation of T-cell antigen receptor/T3 complex mRNA expression in murine T-lymphoma somatic cell hybrids. Proc. Natl. Acad. Sci. USA **83:**6989–6993.
27. **Malissen, M., K. Minard, S. Mjolsness, M. Kronenberg, J. Goverman, T. Hunkapiller, M. B. Prystowsky, Y. Yoshikai, F. Fitch, T. W. Mak, and L. Hood.** 1984. Mouse T cell antigen receptor: structure and organization of constant and joining gene segments encoding the β polypeptide. Cell **37:**1101–1110.
28. **Mattox, W., and B. S. Baker.** 1991. Autoregulation of the splicing of transcripts from the transformer-2 gene of Drosophila. Genes Dev. **5:**786–796.
29. **McDougall, S., C. L. Peterson, and K. Calame.** 1988. A transcriptional enhancer 3′ of $C_{\beta 2}$ in the T cell receptor β locus. Science **241:**205–208.
30. **Mount, S. M.** 1982. A catalogue of splice junctional sequences. Nucleic Acids Res. **10:**459–474.
31. **Nasim, F. H., P. A. Spears, H. M. Hoffmann, H. Kuo, and P. J. Grabowski.** 1990. A sequential splicing mechanism promotes selection of an optional exon by repositioning a downstream 5′ splice site in preprotachykinin pre-mRNA. Genes Dev. **4:**1172–1184.
32. **Padgett, R. A., M. M. Konarska, P. J. Grabowski, S. F. Hardy, and P. A. Sharp.** 1984. Lariat RNA's as intermediates and products in the splicing of messenger RNA precursors. Science **225:**898–903.
33. **Punt, J. A., R. T. Kubo, T. Saito, T. H. Finkel, S. Kathiresan, K. J. Blank, and Y. Hashimoto.** 1991. Surface expression of a T cell receptor β (TCR-β) chain in the absence of TCR-α, -δ, and -γ proteins. J. Exp. Med. **174:**775–783.
34. **Qian, L., M. Vu, M. Carter, and M. F. Wilkinson.** 1992. A spliced intron accumulates as a lariat in the nucleus of T cells. Nucleic Acids Res. **20:**5345–5350.
35. **Qian, L., and M. F. Wilkinson.** 1991. DNA fragment purification: removal of agarose ten minutes after electrophoresis. BioTechniques **10:**736–738.
36. **Rothstein, D. M., H. Saito, M. Streuli, S. F. Schlossman, and C. Morimoto.** 1992. The alternative splicing of the CD45 tyrosine phosphatase is controlled by negative regulatory trans-acting splicing factors. J. Biol. Chem. **267:**7139–7147.
37. **Royer, H. D., and E. L. Reinherz.** 1987. Multiple nuclear proteins bind upstream sequences in the promoter region of a T-cell receptor β-chain variable-region gene: evidence for tissue specificity. Proc. Natl. Acad. Sci. USA **84:**232–236.
38. **Sambrook, J., E. F. Fritsch, and T. Maniatis.** 1989. Molecular cloning: a laboratory manual, 2nd ed. Cold Spring Harbor Laboratory Press, Cold Spring Harbor, N.Y.
39. **Shaw, G., and R. Kamen.** 1986. A conserved AU sequence from the 3′ untranslated region of GM-CSF mRNA mediates selective mRNA degradation. Cell **46:**659–667.
40. **Shimonkevitz, R. P., L. A. Husmann, M. J. Bevan, and I. N. Crispe.** 1987. Transient expression of IL-2 receptor precedes the differentiation of immature thymocytes. Nature (London) **329:**157–159.
41. **Smith, C. W. J., E. B. Porro, J. G. Patton, and B. Nadal-Ginard.** 1989. Scanning from an independently specified branch point defines the 3′ splice site of mammalian introns. Nature (London) **342:**243–247.
42. **Snodgrass, H. R., P. Kisielow, M. Kiefer, M. Steinmetz, and H. von Boehmer.** 1985. Ontogeny of the T-cell antigen receptor within the thymus. Nature (London) **313:**592–595.
43. **Sosnowski, B. A., J. M. Belote, and M. McKeown.** 1989. Sex-specific alternative splicing of RNA from the transformer gene results from sequence-dependent splice site blockage. Cell **58:**449–459.
44. **Takeda, J., A. Cheng, F. Mauxion, C. A. Nelson, R. D. Newberry, W. C. Sha, R. Sen, and D. Y. Loh.** 1990. Functional analysis of the murine T-cell receptor β enhancer and characteristics of its DNA-binding proteins. Mol. Cell. Biol. **10:**5027–5035.
45. **Talerico, M., and S. M. Berget.** 1990. Effect of 5′ splice site mutations on splicing of the preceding intron. Mol. Cell. Biol. **10:**6299–6305.
46. **Tseng, J. C., S. Zollman, A. C. Chain, and F. A. Laski.** 1991. Splicing of the Drosophila P element ORF2-ORF3 intron is inhibited in a human cell extract. Mech. Dev. **35:**65–72.
47. **Wall, R., M. Briskin, C. Carter, H. Govan, A. Taylor, and P. Kincade.** 1986. A labile inhibitor blocks immunoglobulin κ-light-chain-gene transcription in a pre-B leukemic cell line. Proc. Natl. Acad. Sci. USA **83:**295–298.
48. **Wilkinson, M. F.** 1991. Purification of RNA, p. 69–87. *In* T. A. Brown (ed.), Essential molecular biology. Oxford University Press, New York.
49. **Wilkinson, M. F., J. Doskow, and S. Lindsey.** 1990. RNA blots: staining procedures and optimization of conditions. Nucleic Acids Res. **19:**679.
50. **Wilkinson, M. F., J. Doskow, R. von Borstell II, A. M. Fong, and C. L. MacLeod.** 1991. The expression of several T cell-specific and novel genes is repressed by trans-acting factors in immature T lymphoma clones. J. Exp. Med. **174:**269–280.
51. **Wilkinson, M. F., and C. L. MacLeod.** 1988. Induction of T-cell receptor-α and -β mRNA in SL12 cells can occur by transcriptional and post-transcriptional mechanisms. EMBO J. **7:**101–109.
52. **Zeitlin, S., and A. Efstratiadis.** 1984. In vivo splicing products of the rabbit β-globin pre-mRNA. Cell **39:**589–602.
53. **Zhuang, Y., A. M. Goldstein, and A. M. Weiner.** 1989. UACUAAC is the preferred branch site for mammalian mRNA splicing. Proc. Natl. Acad. Sci. USA **86:**2752–2756.